PHYSICAL REVIEW B VOLUME 22, NUMBER 12 15 DECEMBER 1980

Localized states in mixed GaP_zAs_{1-z} crystals

D. Schmeltzer and R. Beserman

Department of Physics, Technion-Israel Institute of Technology, Haifa, Israel
and Solid State Institute, Technion-Israel Institute of Technology, Haifa, Israel

(Received 26 December 1979; revised manuscript received 24 March 1980)

The vibrational properties of a diatomic AB_zC_{1-z} in which the mass m_B and m_C are randomly distributed have been investigated. The calculation has been performed in the short-range-forces approximation. A nonlinear Lagrangian which describes the vibrational properties is obtained by averaging over the random mass. The mass disorder creates a region of continuous localized states near the edge and the center of the averaged crystal Brillouin zone. Experimentally GaP_zAs_{1-z} has been studied by means of Raman scattering; the predicted behavior has been observed which explains the existence of a two-mode behavior in the acoustical region, as well as the appearance of a new peak with LO symmetry in the range of optical frequencies.

I. INTRODUCTION

The purpose of this work is to analyze the vibrational behavior of a diatomic mixed crystal AB_zC_{1-z}. Special attention is paid to the behavior of the phonon density of states close to the band edge. In this region no contribution is usually obtained when the density of states is calculated by the ordinary perturbation method.

The Green's function of the lattice vibration is written as a functional integral, as used by Economou[1] and Nitzan[2] for the problem of the spin-glass. This enables us to calculate subsequently the average phonon density of states.

In order to perform the configurational average of the Green function we use the "replica" or "$n \to 0$" trick.[2,3] The average is performed on a system with a binary probability for the random masses. This way we obtain a nonlinear action. The saddle-point method used by Berezin[4] and Cardy[5] is applied to our case. The nonzero density of states which is obtained is a continuum of localized states in the vicinity of the zone edge and of the zone center.

In order to check the theoretical results from the experimental point of view, we analyze the Raman spectra of GaP_zA_{1-z}. Until now, most of the experimental and theoretical work on mixed crystals has been devoted to the study of the vibrational properties of phonons in the center of the Brillouin zone[6] and comparatively few experiments have been devoted to the study of the vibrational properties near the edge of the Brillouin zone (BZ).[7,8]

For all concentrations z the acoustical part of the Raman spectra of GaP_zAs_{1-z} crystals shows two peaks for the TA branch; one is the virtual-mode frequency and the second is the localized mode. The virtual-crystal vibrations are due to long-range correlation; the localized ones relate to short-range correlation above this frequency. They correspond to the nonzero density of states in accordance with our theoretical calculation. Under the same framework we explain the appearance at low concentration of As of a peak between the LO_Γ and TO_Γ GaP frequencies. It is attributed to the nonzero density of states of the localized mode close to the optical-band edge.

II. FUNCTIONAL REPRESENTATION OF THE GREEN'S FUNCTIONS

In this chapter the lattice-vibration Green's function is written in a functional integral form. We use the $n \to 0$ trick for the calculation of the average Green's function.

The equation of motion for a lattice with two atoms per unit cell l and 3×2 Cartesian coordinates is given by

$$M_\alpha(l)\frac{\partial^2}{\partial t^2}V_\alpha(l,t) = -\sum_{\alpha' l'}\phi_{\alpha\alpha'}(l,l')V_\alpha(l',t)\,. \tag{1}$$

When Fourier transformed, this expression becomes in a matrix form

$$(M\omega^2 - \phi)\,|V\rangle = 0\,, \tag{2}$$

or

$$(\omega^2 - D)\,|u\rangle = 0\,, \tag{3}$$

where D is the dynamical matrix, $|V\rangle$ is the state vector of the displacements, and M is the mass matrix. We have

$$D = M^{-1/2}\phi M^{-1/2}\,, \quad |V\rangle = M^{-1/2}|U\rangle\,.$$

The "mass-weighted" displacement Green's function, which gives the density of states, is the inverse of the dynamical matrix[9]

$$G_{\alpha\alpha'}(l,l',\omega^2) = (\omega^2 - D)^{-1}_{\alpha\alpha',ll'}\,, \tag{4}$$

which can be written as a functional integral (see the Appendix)

$$G_{\alpha\alpha'}(l,l',\omega^2)=Z^{-1}\int[du]u_\alpha(l)u_{\alpha'}(l')\exp[-S(u)]\,, \tag{5}$$

where

$$[du]=d^3u_1(l=1)d^3u_2(l=1),\ldots,\\ d^3u_1(l=N^3)d^3u_2(l=N^3)\,, \tag{6}$$

$$S(u)\equiv\tfrac{1}{2}\sum_{\alpha l,\alpha' l'}u_\alpha(l)(\omega^2-D)_{\alpha l,\alpha' l'}u_{\alpha'}(l')\,, \tag{7}$$

and

$$Z\equiv\int[du]\exp[-S(u)]\,. \tag{8}$$

We introduce for every displacement an n-component field

$$|u_\alpha(l)\rangle=[u_\alpha^{(1)}(l),\ldots,u_\alpha^{(r)}(l),\ldots,u_\alpha^{(n)}(l)]\,, \tag{9}$$

and the two-points correlation function becomes

$$\begin{aligned}G_{\alpha\alpha'}(l,l',\omega^2)&=\lim_{n\to0}\int[du]u_\alpha(l)u_{\alpha'}(l')\exp[-S(u)]Z^{n-1}\\&=\lim_{n\to0}\int[\mathfrak{D}(u)]u_\alpha(l)u_{\alpha'}(l')\\&\qquad\times\exp\left(-\sum_{r=1}^{n}S(u^{(r)})\right)\,,\end{aligned} \tag{10}$$

where

$$[\mathfrak{D}(u)]\equiv[du^{(1)}]\cdots[du^{(n)}] \tag{11}$$

and

$$Z^n=\int[\mathfrak{D}(u)]\exp\left(-\sum_{r=1}^{n}S(u^{(r)})\right)\,. \tag{12}$$

This is the $n\to0$ trick[2,3] which has been used before for electrons in a random potential. At this stage we are able to calculate the averaged Green's function which will be done in the next section.

III. AVERAGED GREEN'S-FUNCTION CALCULATION

In order to perform the configurational average on the Green's function we introduce a probability distribution for the random mass M_2 which takes two values M_B and M_C. The mass M_1 is fixed and has the value M_A.

We assume the following probability distribution:

$$\mathcal{P}(M_2(l);l=1,2,\cdots)=\prod_{l=1}^{N^3}P(M_2(l))\,, \tag{13}$$

where

$$P(M_2(l))=z\delta_{M_2(l),M_B}+(1-z)\delta_{M_2(l),M_C}\,. \tag{14}$$

z is the concentration of M_B and $1-z$ is the concentration M_C. With this probability distribution, the configurational average for the two-point correlation function is (until now it was convenient to use α to label both the atom and the Cartesian coordinates but from now on we have to separate the two; α will label the Cartesian coordinate and s specifies the atoms)

$$\begin{aligned}\langle G_{\alpha\alpha'}(l,l';s,s';\omega^2)\rangle=\lim_{n\to0}\int[\mathfrak{D}(u)]u_\alpha(l,s)u_{\alpha'}(l',s')\exp&\left(-\tfrac{1}{2}\sum_{\alpha,l,s;\alpha',l',s';r}u^{(r)}(l',s)\omega^2u_{\alpha'}^{(r)}(l',s')\right)\\ \times\exp&\left(\tfrac{1}{2}\sum_{\alpha,l;\alpha',l',r}u_\alpha^{(r)}(l,1)D_{\alpha\alpha'}(l,l';1,1)u_{\alpha'}^{(r)}(l',1)\right)\\ \times\prod_{l=1}^{N^3}\Bigg[z\exp&\left(\tfrac{1}{2}\sum_{\alpha,l,r}u_\alpha^{(r)}(l,2)\frac{\phi_{\alpha\alpha'}(l,l;22)}{M_B(l)}u_\alpha^{(r)}(l,2)\right.\\&\left.\quad-\tfrac{1}{2}\sum_{\alpha,l;\alpha',l',r}u_\alpha^{(r)}(l,2)\frac{\phi_{\alpha\alpha'}(l,l';2,1)}{[M_B(l)M_A(l')]^{1/2}}u_{\alpha'}^{(r)}(l',1)\right)\\ +(1-z)\exp&\left(\tfrac{1}{2}\sum_{\alpha,l,r}u_\alpha^{(r)}(l,2)\frac{\phi(l,l;2,2)}{M_C(l)}u_\alpha^{(r)}(l,2)\right.\\&\left.\quad+\tfrac{1}{2}\sum_{\alpha,l;\alpha',l',r}u_\alpha^{(r)}(l,2)\frac{\phi_{\alpha\alpha'}(l,l';2,1)}{[M_C(l)M_A(l')]^{1/2}}u_\alpha^{(r)}(l',1)\right)\Bigg]\,.\end{aligned} \tag{15}$$

We consider only the nearest-neighbor interaction; with this approximation the averaged Green's function takes a simple form. The next-nearest neighbors have second-order influence on the averaged Green's function. The multiplicative factor z and $(1-z)$ might be written in exponential form and expression (15) becomes in a symmetric form

$$
\begin{aligned}
\langle G_{\alpha\alpha'}(l,l';s,s';\omega^2)\rangle = \lim_{n\to 0}\int [\mathfrak{D}(u)]u_\alpha(l,s)u_{\alpha'}(l',s') \\
\times \exp\left(-\tfrac{1}{2}\sum_{\alpha,l,s;\alpha',l',s',r} u_\alpha^{(r)}(l,s)[\omega^2 - D^0_{\alpha\alpha'}(l,l';s,s')]u_{\alpha'}^{(r)}(l',s')\right) \\
\times \exp\left\{\sum_l \ln\cosh\left[\tfrac{1}{2}\sum_{\alpha,\alpha',r} u_\alpha^{(r)}(l,2)\phi_{\alpha\alpha'}(l,l';2,2)\frac{1}{2}\left(\frac{1}{M_B}-\frac{1}{M_C}\right)u_\alpha^{(r)}(l,2)\right.\right. \\
+\tfrac{1}{2}\sum_{\alpha,\alpha',l',r} u_\alpha^{(r)}(l,2)\frac{1}{2}\,\frac{\phi_{\alpha\alpha'}(l,l';2,1)}{\sqrt{M_A}} \\
\left.\left.\times\left(\frac{1}{\sqrt{M_B}}-\frac{1}{\sqrt{M_C}}\right)u_{\alpha'}^{(r)}(l',1)+\tfrac{1}{2}\ln\left(\frac{z}{1-z}\right)\right]\right\}. \qquad (16)
\end{aligned}
$$

$s=1$ represents the mass M_A and $s=2$ is the mass M_B or M_C. $D^0_{\alpha\alpha'}(l,l';s,s')$ is given by

$$
D^0_{\alpha\alpha'}(l,l';s,s')=\begin{cases}
\dfrac{\phi_{\alpha\alpha'}(l,l';1,1)}{M_A}, & s=s'=1 \\[2ex]
\dfrac{\phi_{\alpha\alpha'}}{\sqrt{M_A}}(l,l';1,2)\dfrac{1}{2}\left(\dfrac{1}{\sqrt{M_B}}+\dfrac{1}{\sqrt{M_C}}\right), & s=1, s'=2 \\[2ex]
\phi_{\alpha\alpha'}(l,l';2,2)\dfrac{1}{2}\left(\dfrac{1}{M_B}+\dfrac{1}{M_C}\right), & s=s'=2 .
\end{cases} \qquad (17)
$$

We note that in the one-dimensional case the nonlinear part of the effective action takes a simple form:

$$
\sum_l \ln\cosh\tfrac{1}{2}\sum_{r=1}^{n}\left[K\Delta_1 u_{2,l}^{(r)^2} - 2G\Delta_2 u_{2,l}^{(r)}(u_{1,l}^{(r)}+u_{1,l+1}^{(r)}) - (K-G)u_{1,l}^{(r)}u_{2,l}^{(r)} + \ln\left(\frac{z}{1-z}\right)\right], \qquad (18)
$$

where K is the force constant between atoms in the unit cell l and G is the force constant between atoms in the cells l and $(l+1)$; Δ_1 and Δ_2 are defined by

$$
\Delta_1=\frac{1}{2}\left(\frac{1}{M_B}-\frac{1}{M_C}\right), \quad \Delta_2=\frac{1}{2\sqrt{M_A}}\left(\frac{1}{\sqrt{M_B}}-\frac{1}{\sqrt{M_C}}\right). \qquad (19)
$$

The effective action can be written

$$
\begin{aligned}
S_{\text{eff}} = \sum_{q,j,r}\tfrac{1}{2}[\omega^2-\omega_j^2(q)]u_j^{(r)2}(q) - \sum_l \ln\cosh\left[\tfrac{1}{2}\sum_{\alpha,r}u_\alpha^{(r)}(l,2)\phi_{\alpha\alpha}(l,l;2,2)\Delta_1 u^{(r)}(l,2)\right. \\
\left. +\tfrac{1}{2}\sum_{\alpha,\alpha',l',r}u_\alpha^{(r)}(l,2)\phi_{\alpha\alpha'}(l,l';2,1)\Delta_2 u_{\alpha'}^{(r)}(l',1)+\tfrac{1}{2}\ln\left(\frac{z}{1-z}\right)\right],
\end{aligned} \qquad (20)
$$

where $\vec{q}$ is the wave vector, j applies to either the optical or to the acoustical mode, and $\omega_j^2(q)$ is the eigenfrequency of the virtual lattice defined in terms of the dynamical matrix,

$$
(\omega^2 - D^0)|u\rangle = 0 . \qquad (21)
$$

The nonlinear part of the action contains the deviation from the virtual (averaged) lattice. At this stage we write the effective action in the continuous representation at the center and at the edge of the Brillouin zone. We neglect terms which contain derivatives higher than ∇^2 and we assume that there are no interactions between modes. With these approximations we are able to write the effective action for every mode.

$$
S_{\text{eff}} = \int dX^d \sum_{r=1}^{n}\{a^{-d}a^2\gamma_J\tfrac{1}{2}[\nabla u_J^{(r)}(x)]^2 + \tfrac{1}{2}a^{-d}(\omega^2-\omega_J^2)(u_J^{(r)2}(x)\} - a^{-d}\ln\cosh\left[\tfrac{1}{2}\sum_{r=1}^{n}\lambda_J u_J^{(r)2}(x) + \tfrac{1}{2}\ln\left(\frac{z}{1-z}\right)\right]. \qquad (22)
$$

a is the lattice spacing, d is the dimensionality of the lattice, and the factor a^{-d} comes from the conversion of the sum over sites into an integral (a^d—the volume of the unit cell in d dimensions).

$$
\sum_l F(u(l)) = \int dX^d a^{-d} F(u(x)) . \qquad (23)
$$

γ_J is the constant which takes into consideration the bending of the band at the edge or at the center of the Brillouin zone with momentum q_0.

$$\omega_J^2(q) = \omega_J^2(q_0) + \tfrac{1}{2}\gamma_J(q-q_0)^2 .$$

γ_J is negative for zone-edge optical phonons and for zone-center acoustical phonons; it is positive for zone-edge acoustical phonons and for zone-center optical phonons. The factor $\frac{1}{2}\ln[z/(1-z)]$ expresses the shift of the band edge as a function of the concentration. λ_J is the coupling constant which expresses the deviation from the virtual crystal. Its value is of the order of magnitude of half of the square-root difference between the pure crystals' band-edge frequencies.

A numerical estimation can be made for the λ_J parameter. We assume a lattice-dynamic model with two force constants. With this model we can calculate the ratio of the vibration amplitude between the two atoms for a given mode in the virtual crystal. From this ratio we can estimate the value of λ_J for every mode.

In order to simplify the discussion we scale the displacement of the atoms in the following way:

$$u(x) \to yu(x) \quad \text{with } y^2\gamma_J a^{2-d} = 1 , \tag{24}$$

$$S_{\text{eff}} = \int dx^d \sum_{r=1}^{n} \tfrac{1}{2}\left[(\nabla u_J^{(r)})^2 + (\omega^2 - \omega_J^2)\gamma_J^{-1}a^{-2}u_J^{(r)2}\right] - a^{-d}\ln\cosh\left[\tfrac{1}{2}\lambda_J\gamma_J^{-1}a^{d-2}\sum_{r=1}^{n} u_J^{(r)2} + \tfrac{1}{2}\ln\left(\frac{z}{1-z}\right)\right] . \tag{25}$$

The autocorrelation is given by the imaginary part of the two-point correlation function when ω^2 is replaced by $\omega^2 + i\epsilon$

$$\langle \text{Im}G(x,x';\omega^2+i\epsilon)\rangle = \text{Im} \lim_{n\to 0,\epsilon\to 0} \int [\mathfrak{D}(u)]u(x)u(x_1) \times \exp[-S_{\text{eff}}(x)] . \tag{26}$$

We note that if we perform the ordinary loop expansion for $(\omega^2 - \omega_J^2)\gamma_J^{-1} < 0$, each term in the perturbation expansion is nonsingular as $\epsilon \to 0$. This means that to any order in the perturbation theory the density of state is zero. It is expected that the density of states would be nonzero in the region of localized states; the perturbation series must diverge enormously, and this divergence is controlled by the existence of a nontrivial solution of the effective action. We look for the existence of nontrivial saddle points $u_c^{(r)}(x)$ of S_{eff}:

$$\left.\frac{\delta S_{\text{eff}}}{\delta u^{(r)}}\right|_{u_c^{(r)}} = 0 . \tag{27}$$

We can write

$$u^{(r)}(x) = u_c^{(r)}(x) + \eta(x) , \tag{28}$$

$$S_{\text{eff}} = S_{\text{eff}}(u_c) + \tfrac{1}{2}\delta^2 S . \tag{29}$$

$u_c^{(r)}(x)$ satisfies the following equation:

$$-\nabla^2 u_c^{(r)} + (\omega^2 - \omega_J^2)\gamma_J^{-1}a^{-2}u_c^{(r)} - \lambda_J a^{-2}\gamma_J^{-1}\tanh\left[\tfrac{1}{2}\lambda_J\gamma_J^{-1}a^{d-2}\sum_{r=1}^{n} u^{(r)2} + \tfrac{1}{2}\ln\left(\frac{z}{1-z}\right)\right]u_c^{(r)} = 0 . \tag{30}$$

When we look for a wavelike solution we find a region which corresponds to an unstable wave. This wave can be interpreted as a localized mode. Equation (30) is satisfied for every one of the r components of $u_c^{(r)}$. We have for $u_c(x)$

$$-\nabla^2 u_c(x) + (\omega^2 - \omega_J^2)\gamma_J^{-1}a^{-2}u_c(x) - \lambda_J a^{-2}\gamma_J^{-1}\tanh\left[\tfrac{1}{2}\lambda_J\gamma_J^{-1}a^{d-2}u_c^2(x) + \tfrac{1}{2}\ln\left(\frac{z}{1-z}\right)\right]u_c(x) = 0 . \tag{31}$$

In the rest of this section we give a qualitative analysis of this equation and we perform explicitly the calculations for the density of states.

We start our discussion with the transverse-acoustic mode of the zone edge. It was seen experimentally that in GaP_zAs_{1-z} and in ZnS_zSe_{1-z} we have a two-mode behavior for the TA(X) zone-edge phonon. We substitute the parameter λ_{TA} and $\tilde{\omega}_{TA}^2$ [$\tilde{\omega}_{TA}^2$ is the frequency calculated for concentration $z = 0.5$ in the virtual-crystal approximation (VCA)].

For $u_c(x) \neq 0$ we write Eq. (31) in the form

$$-\frac{\nabla^2 u_c(x)}{u_c(x)} = -\lambda_{TA}a^{-2}\gamma_{TA}^{-1} \times \left\{\frac{\omega^2 - \omega_{TA}^2}{\lambda_{TA}} - \tanh\left[\tfrac{1}{2}\lambda_{TA}\gamma_{TA}^{-1}a^{d-2}u_c^2(x) + \tfrac{1}{2}\ln\left(\frac{z}{1-z}\right)\right]\right\} \tag{32}$$

(for the TA mode γ_{TA}^{-1} is positive).

In the Wentzel-Kramers-Brillouin (WKB) approximation, $-\nabla^2 u_c(x)/u_c(x)$ is equal to the square of the momentum. For $-\nabla^2 u_c(x)/u_c(x) < 0$ we have a damped wave in space which happens for frequencies

$$\omega^2 > \omega_{TA}^2 + \lambda_{TA} . \tag{33}$$

$-\nabla^2 u_c(x)/u_c(x) > 0$ corresponds to a traveling wave and this is satisfied for frequencies

$$\omega^2 < \omega_{TA}^2 + \lambda_{TA}\tanh\left[\tfrac{1}{2}\ln\left(\frac{z}{1-z}\right)\right] . \tag{34}$$

In addition we have the interesting region where $-\nabla^2 u_c(x)/u_c(x)$ can be positive or negative, which corresponds to unstable wave propagation; this takes place in the frequency range

$$\tilde{\omega}_{\mathrm{TA}}^2 + \lambda_{\mathrm{TA}} \tanh\left[\tfrac{1}{2}\ln\left(\frac{z}{1-z}\right)\right] < \omega^2 < \omega_{\mathrm{TA}}^2 + \lambda_{\mathrm{TA}} \,. \qquad (35)$$

We define $\omega^2_{\mathrm{TA_{VCA}}}$ as

$$\omega^2_{\mathrm{TA_{VCA}}} = \tilde{\omega}_{\mathrm{TA}}^2 + \lambda_{\mathrm{TA}} \tanh\left[\tfrac{1}{2}\ln\left(\frac{z}{1-z}\right)\right] . \qquad (36)$$

This corresponds to the maximum propagating frequency.

In the range of frequencies given by Eq. (35) (the range of unstable wave propagation) we have solutions u_0 which correspond to $\nabla^2 u_c(x) = 0$ and $u_c(x) \neq 0$. u_0 is the solution of

$$\frac{\omega^2 - \tilde{\omega}_{\mathrm{TA}}^2}{\lambda_{\mathrm{TA}}} = \tanh\left[\tfrac{1}{2}\lambda_{\mathrm{TA}}\gamma_{\mathrm{TA}}^{-1} a^{d-2} u_0^2(x) + \tfrac{1}{2}\ln\left(\frac{z}{1-z}\right)\right] . \qquad (37)$$

The value of u_0^2 can be found graphically from the tanh curve which tends toward 1 when $u_c^2(x)$ tends toward $+\infty$.

The region of unstable wave propagation is interpreted as a region of localized nature. (For a given frequency we have regions where the wave propagates and others where the wave is damped.) It is seen that for $u_c^2(x) > u_0^2$, $-\nabla^2 u_c(x)/u_c(x) > 0$ and for $u_c^2(x) < u_0^2$, $-\nabla^2 u_c(x)/u_c(x) < 0$.

For $(\omega^2 - \tilde{\omega}_{\mathrm{TA}}^2)/\lambda_{\mathrm{TA}} \approx 1$, $u_0^2 \to \infty$ in the approximation considered here, we have $\nabla^2 u_c = 0$. This means that in addition to the VCA mode at $\tilde{\omega}_{\mathrm{TA}}^2 + \lambda_{\mathrm{TA}} \ln[z/(1-z)]$, when ω^2 is close to $\tilde{\omega}_{\mathrm{TA}}^2 + \lambda_{\mathrm{TA}}$ we have a new mode corresponding to the zone edge at $q = q_0$. For zone center $q = 0$ corresponds to the ordinary local mode. A similar derivation can be used for the optical bands and we obtain qualitatively similar results.

An explicit calculation of the density of states can be performed which will be limited to the following range of frequencies:

(a) $\left|\dfrac{\omega^2 - \tilde{\omega}_J^2}{\lambda_J}\right| \approx 1$, $u_0^2 \to \infty$

(b) $\left|\dfrac{\omega^2 - \tilde{\omega}_J^2}{\lambda_J}\right| \ll 1$, $u_0^2 \to 0$

(c) intermediate range.

In case (a), $\ln\cosh[f(x)] \approx f(x)$ and we obtain the following action:

$$S_{\mathrm{eff}} \approx \int dx^d \left(\sum_{r=1}^{n} \tfrac{1}{2}\left[(\nabla u^{(r)})^2 + (\omega^2 - \tilde{\omega}_J^2 - \lambda_J)\gamma_J^{-1} a^{-2} u^{(r)^2}\right]\right) , \qquad (38)$$

giving a finite density of states close to $\omega^2 \approx \tilde{\omega}_J^2 + \lambda_J$, which corresponds to the local or gap modes. For case (b) we use the expansion of $\ln\cosh[f(x) + a_0]$:

$$\ln\cosh[f(x) + a_0] \approx \ln\cosh(a_0) + \tanh(a_0) f(x) + \tfrac{1}{2}\,\mathrm{sech}^2(a_0) f(x)^2$$

giving the action

$$S_{\mathrm{eff}} \approx \int dx^d \left[\tfrac{1}{2}\sum_{r=1}^{n} (\nabla u^{(r)})^2 - \tfrac{1}{2}\Omega^2 \sum_{r=1}^{n} u^{(r)^2} - \tfrac{1}{4} g \left(\sum_{r=1}^{n} u^{(r)^2}\right)^2\right] , \qquad (39)$$

where

$$-\Omega^2 \equiv \left\{\omega^2 - \tilde{\omega}_J^2 - \lambda_J \tanh\left[\tfrac{1}{2}\ln\left(\frac{z}{1-z}\right)\right]\right\}\gamma_J^{-1} a^{-2} \qquad (40)$$

and

$$g \equiv \lambda_J^2 \gamma_J^{-2} a^{d-4}\,\mathrm{sech}^2\left[\tfrac{1}{2}\ln\left(\frac{z}{1-z}\right)\right] . \qquad (41)$$

The action (39) is used to calculate the density of states for $\Omega^2 < 0$ close to the edge or to the center of the Brillouin zone. We follow the method of perturbation at large order used in Ref. 4 and write

$$\langle G(x,x')\rangle = \sum_{k=0}^{\infty} g^k \langle G\rangle_k , \qquad (42)$$

where $\langle G\rangle_k$ is the kth order of $\langle G\rangle$ which is given by

$$\langle G(x,x';\Omega^2 + i\epsilon)\rangle_k = \frac{1}{2i\pi}\oint \frac{dg}{g^{k+1}} \int [\mathfrak{D}(u)]\, u(x) u(x') \times \exp(-S_{\mathrm{eff}}) . \qquad (43)$$

We calculate the saddle point in the space of g and $u(x)$,

$$\frac{k}{g_c} = \tfrac{1}{4}\int dx^d u_c^4(x)$$
$$(-\nabla^2 - \Omega^2) u_c(x) = g u_c^3(x) , \qquad (44)$$

where

$$u_c = (u_c^{(1)} \cdots u_c^{(r)} \cdots u_c^{(n)}) . \qquad (45)$$

At the saddle point we obtain for the effective action

$$S_{\mathrm{eff}}(u_c) = -\frac{\Omega^{4-d}}{g} C_d , \qquad (46)$$

$$u_c(x) \equiv \frac{|\Omega|}{\sqrt{g}} V_c(|\Omega| x) , \qquad (47)$$

$$C_d = \tfrac{1}{4}\int V_c^4(x) d^d x . \qquad (48)$$

To evaluate the leading contribution to $\mathrm{Im}\langle G(x,x';\Omega^2+i\epsilon)\rangle$ near the saddle point, we integrate over the fluctuations in its vicinity. We write $u(x)=u_c(x)+\eta(x)$ and we keep the term $O(\eta^2)$ in the action. Before carrying out the Gaussian integration over η we must separate out the zero modes. This is done using the transformation to the collective coordinate introduced by Langher[10] and by Christ and Lee.[11] Following the treatment of Ref. 4 we obtain

$$\begin{aligned}\mathrm{Im}\langle G(x,x';\Omega^2+i\epsilon)\rangle_{\epsilon\to 0,n\to 0}\\ \approx(-\Omega^2)^{d/2-1}b^{-(d+1)/2}\\ \times\exp\left(\frac{-C_d}{b}\right)\int V_c(x-x_0)V_c(x'-x_0)d^dx_0\,,\end{aligned}\tag{49}$$

where

$$b\equiv\frac{g}{(-\Omega^2)^{2-d/2}}\,,\tag{50}$$

for $d=3$ we have

$$\begin{aligned}\mathrm{Im}\langle G(x,x';\Omega^2+i\epsilon)\rangle_{\epsilon\to 0,n\to 0}\\ \approx(-\Omega^2)^{3/2}g^{-2}\exp\left(-\frac{C_d}{g}(-\Omega^2)^{1/2}\right)\\ \times\int V_c(x-x_0)V_c(x'-x_0)d^3x_0\,.\end{aligned}\tag{51}$$

In case (c), in order to calculate the density of states for frequencies in the range

$$\tilde{\omega}_J^2+\lambda_J\tanh\left[\tfrac{1}{2}\ln\left(\frac{z}{1-z}\right)\right]<\omega^2<\tilde{\omega}_J^2+\lambda_J\,,$$

we linearized Eq. (37) around the point $\pm u_0$. We calculate up to the second order:

$$\begin{aligned}\ln\cosh\left[\tfrac{1}{2}\lambda_J\gamma_J^{-1}a^{d-2}\sum_r\left[\pm u_0^{(r)}(x)+(u^{(r)}\mp u_0^{(r)})\right]^2\right.\\ \left.+\tfrac{1}{2}\ln\left(\frac{z}{1-z}\right)\right]\\ -\ln\cosh\left[\tfrac{1}{2}\lambda_J\gamma_J^{-1}a^{d-2}\sum_{r=1}^{n}u_0^{(r)2}+\tfrac{1}{2}\ln\left(\frac{z}{1-z}\right)\right].\end{aligned}$$

The action for this case takes the form

$$S_{\mathrm{eff}}=\int d^dx\left[\tfrac{1}{2}\sum_{r=1}^{n}(\nabla u^{(r)2}-\tfrac{1}{2}\tilde{\Omega}^2u^{(r)2})-\tfrac{1}{4}\tilde{g}\left(\sum_{r=1}^{n}u^{(r)2}\right)^2\right],\tag{52}$$

where

$$-\tilde{\Omega}^2=\lambda_J^2\gamma_J^{-2}a^{d-4}\,\mathrm{sech}^2\left[\lambda_J\gamma_J^{-1}a^{d-2}u_0^2+\tfrac{1}{2}\ln\left(\frac{z}{1-z}\right)\right]u_0^2\,,\tag{53}$$

$$\tilde{g}=\lambda_J^2\gamma_J^{-2}a^{d-4}\,\mathrm{sech}^2\left[\lambda_J\gamma_J^{-1}a^{d-2}u_0^2+\tfrac{1}{2}\ln\left(\frac{z}{1-z}\right)\right].\tag{54}$$

The density of states calculated with (52) gives the same results as given by (51) with parameter $\tilde{\Omega}^2$ and $\tilde{g}$ instead of Ω^2 and g.

The existence of the band tail at the zone edge explains the appearance of the Raman peak between the TO_Γ and LO_Γ of GaP at small concentrations of As. This experimental fact will be analyzed in Sec. IV.

In order to check the validity of our model, we compare our results to those of Maradudin.[12] In the $\Omega^2>0$ range we can use the ordinary loop expansion; considering the action given by Eq. (44) we obtain a small correction to the density of states.

Then we study the lifetime of the phonon close to the center and to the edge of the Brillouin zone and compare with the results of Ref. 12. In order to calculate the phonon lifetime we write the action given in Eq. (43) in the momentum representation.

We calculate the self-energy[13] of the phonon up to the second order. [The calculations are identical to those given in Ref. 13 for a u^4 field with $O(n)$ symmetry.]

The self-energy up to the second order is

$$\Sigma(\Omega^2+i\epsilon)=(n+2)g'D_1(\Omega^2,a^{-1})\,,\tag{55}$$

where

$$g'\equiv\frac{g}{\gamma_J^{-1}a^{-2}}=\lambda_J^2\gamma_J^{-1}a^{d-2}$$

and

$$D_1(\Omega^2,a^{-1})=\int_0^{a^{-1}}\frac{d^dq}{q^2-\Omega^2}\,.\tag{56}$$

The lifetime τ is given by

$$\tau^{-1}=\mathrm{Im}\Sigma(\Omega^2+i\epsilon)_{\epsilon\to 0,n\to 0}=2\pi g'\int d^dq(q^2-\Omega^2)\,.\tag{57}$$

Evaluating Eq. (57) we obtain

$$\tau^{-1}=\mathrm{Im}\Sigma(\Omega^2+i\epsilon)_{\epsilon\to 0,n\to 0}=\begin{cases}\pi g'(\Omega^2)^{1/2}, & d=3\\ \pi g'(\Omega^2)^{-1/2}, & d=1\,.\end{cases}\tag{58}$$

We compare our result to those obtained by Maradudin[12] for $d=1$.

$$\tau^{-1}=\mathrm{Im}\Sigma(\omega^2+i\epsilon)_{\epsilon\to 0}\approx\mu_2\tilde{\omega}_J^4(|\omega^2-\tilde{\omega}_J^2|)^{-1/2}\,,\tag{59}$$

where μ_2 is given by

$$\begin{aligned}\mu_2=z\left(\frac{[zM_B^{-1}+(1-z)M_C^{-1}]^{-1}}{M_B}-1\right)^2\\ +(1-z)\left(\frac{[zM_B^{-1}+(1-z)M_C^{-1}]^{-1}}{M_C}-1\right)^2.\end{aligned}\tag{60}$$

Comparing the two results after introducing the explicit value of g we see a good agreement. In fact Eq. (59) can be used to fit λ_J instead of using the model given in Ref. 8.

In order to compare Maradudin's results to ours we shall take the simple case $z = 0.5$. In our theory the mean-square frequency deviation λ_J is of the order $\lambda_J \approx \sqrt{\mu_2}\, \omega_J^2$ and from (58)

$$\tau^{-1} = \pi g' / (\Omega^2)^{1/2} = \pi\lambda_J^2(|\omega^2 - \omega_J^2|)^{-1/2} ,$$

which is in agreement with Eq. (59).

IV. RAMAN SCATTERING (RS) BY MIXED GaP_zAs_{1-z} CRYSTALS

These crystals were epitaxial deposited layers, the substrate being GaP for GaP-rich crystals and GaAs for GaAs-rich materials. The Raman spectra were obtained with a Spex triple monochromator; the 4880-Å line of argon was chosen because its penetration depth was smaller than the thickness of the layer. In order to improve the RS efficiency the laser light penetrates the layer at an angle close to the Brewster angle. Experiments were performed at room temperature and at 2 K for most of the crystals.

Figure 1 shows the room-temperature spectra of GaP, $GaP_{0.8}As_{0.2}$, $GaP_{0.2}As_{0.4}$, $GaP_{0.35}As_{0.65}$, and GaAs. The GaP and GaAs spectra are identical to those previously published. When GaP and GaAs are mixed we observe the two-mode behavior of the zone-center phonons. The zone-edge optical phonons exhibit a typical two-mode behavior, the GaP-like and the GaAs-like peaks without any cross combinations between GaP and GaAs. These results are in accordance with the infrared results.[7]

In pure GaAs and pure GaP the combination of acoustical phonons generates a $2\omega_{TA(X)}$ (GaAs) peak at 158 cm^{-1} and a $2\omega_{TA(X)}$ (GaP) peak at 214 cm^{-1}, respectively. In mixed crystals for all concentrations, two peaks are seen in the frequency range of combination between acoustical phonons. The first peak exhibits a concentration dependence; for $z = 0.6$, $2\omega_{TA} = 180$ cm^{-1}; for $z = 0.35$, $2\omega_{TA} = 172$ cm^{-1}. The second one does not shift appreciably with concentration for $z = 0.6$, $2\omega_{TA} = 210$ cm^{-1}; for $z = 0.35$, $2\omega_{TA} = 206$ cm^{-1}.

These experimental results can be understood in the framework of the theory presented in the previous sections. The nonlinear action given by Eq. (25) is used to calculate the density of states, and we integrate the Gaussian fluctuations around the stationary points. The total contribution is the sum of the integrations around all these points. One contribution is given by $\nabla^2 u = 0$; it fulfills case (a) and from Eq. (38), it is important only when

$$|(\omega^2 - \omega_j^2)/\lambda_j| \simeq 1 .$$

A second contribution is obtained from case (b), the solution of Eq. (47) and gives a contribution to the density of states given by Eq. (49).

For the sake of simplicity, we shall explicitly analyze the crystal $GaP_{0.5}As_{0.5}$, the action for other concentrations can be deduced according to Eq. (25). For this case, the action takes the form

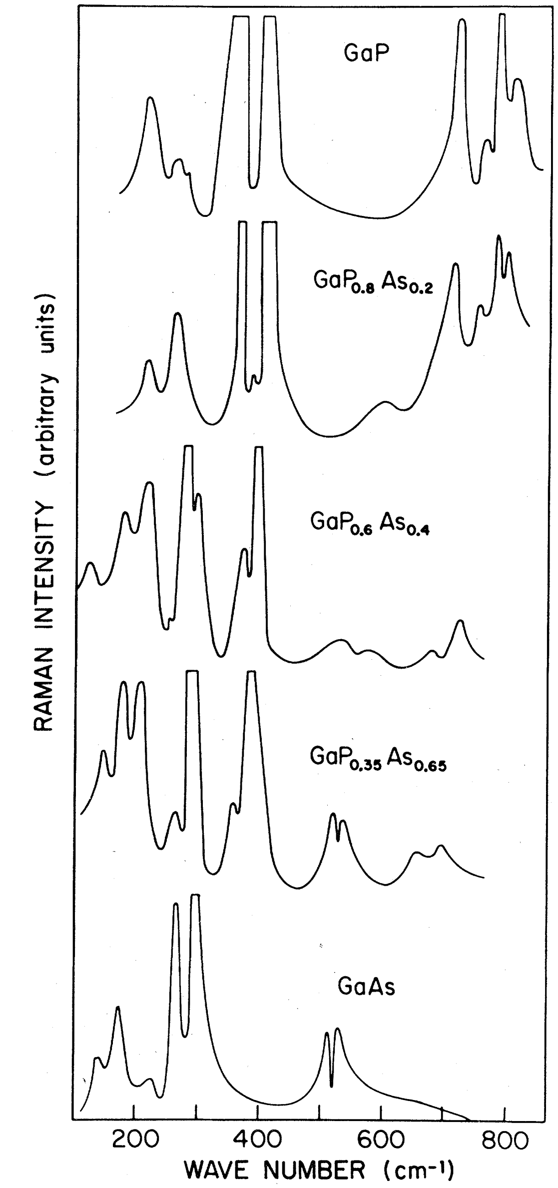

FIG. 1. Room-temperature Raman spectra of mixed GaP_zAs_{1-z} for concentrations $z = 1$, 0.8, 0.6, 0.35, and 0.

$$S_{\mathrm{eff}}=\int d^3x \sum_{r=1}^{n}\left[\tfrac{1}{2}\nabla u_{\mathrm{TA}}^{(r)^2}(x)+(\omega^2-\tilde{\omega}_{\mathrm{TA}}^2)\gamma_{\mathrm{TA}}^{-1}a^{-2}u_{\mathrm{TA}}^{(r)^2}(x)\right]$$

$$-a^{-3}\ln\cosh\left(\tfrac{1}{2}\lambda_{\mathrm{TA}}\,\gamma_{\mathrm{TA}}^{-1}\,a\sum_{r=1}^{n}u_{\mathrm{TA}}^{(r)^2}(x)\right)\ .$$

According to case (a) and to Eq. (38), the local mode will appear when

$$\omega^2=\omega_{\mathrm{TA}}^2+\lambda_{\mathrm{TA}}\ .$$

In order to compare this frequency with the experimental results we have to evaluate λ_{TA}. In the unit cell, the Ga atoms occupy site 1, and site 2 is occupied by P(As) atoms.

The zone-edge phonon frequencies can be obtained using a one-dimensional model with two force constants. The nonlinear part of the action is given by Eq. (18). The coupling constants K and G are expressed, respectively, as the sum and the difference of two force constants A and B, which will be deduced from the experimental frequencies of GaP (GaAs) at the X point; A and B are not concentration dependent. At the edge of the BZ the frequencies and the displacement vectors are the solution of

$$\begin{pmatrix}\omega^2-\dfrac{4A}{M_1} & \dfrac{4B}{M_2}\\[2ex] \dfrac{4B}{M_1} & \omega^2-\dfrac{4A}{M_2}\end{pmatrix}\begin{pmatrix}\bar{l}_1\\[2ex] \bar{l}_2\end{pmatrix}=0\ .$$

The transverse frequencies are

$$\omega_{\mathrm{TO,TA}}^2=2A\left(\frac{1}{M_1}+\frac{1}{M_2}\right)$$

$$\pm\left[4A^2(M_1^{-1}-M_2^{-1})^{2}+16B^2M_1^{-1}M_2^{-1}\right]^{1/2}\ .$$

The displacements are

$$U_{\mathrm{TO}}=\tfrac{1}{2}(\bar{l}_1-\bar{l}_2)\ ,$$

$$U_{\mathrm{TA}}=\tfrac{1}{2}(\bar{l}_1+\bar{l}_2)\ .$$

At the X point the longitudinal frequencies correspond to the linear chain with only the force constant $A\neq 0$ and $B=0$.

From the $\omega_{\mathrm{TO}(X)}(\mathrm{GaP})=367\ \mathrm{cm}^{-1}$ and $\omega_{\mathrm{TA}(X)}(\mathrm{GaP})=105\ \mathrm{cm}^{-1}$ we can deduce A and B:

$$A=7.5\times10^5\ \mathrm{sec}^{-2}(\mathrm{a.u.})\ ,$$

$$B=6.6\times10^5\ \mathrm{sec}^{-2}(\mathrm{a.u.})\ .$$

Under these approximations the average VCA frequency is

$$\tilde{\omega}_{\mathrm{TA}}^2=2A\left(\frac{1}{m_{\mathrm{Ga}}}+\frac{1}{m_2}\right)$$

$$-\left[4A^2(m_{\mathrm{Ga}}^{-1}-m_2^{-1})^2+16B\,m_{\mathrm{Ga}}^{-1}m_2^{-1}\right]^{1/2}$$

$$=(85\ \mathrm{cm}^{-1})^2\ ,$$

with

$$\frac{1}{m_2}=\frac{1}{2}\left(\frac{1}{m_{\mathrm{P}}}+\frac{1}{m_{\mathrm{As}}}\right)\ ,$$

and

$$\lambda_{\mathrm{TA}}=\left(1+\frac{\bar{l}_1}{\bar{l}_2}\right)^{-2}\left[2(A+B)\Delta_1-8B\Delta_2\left(\frac{\bar{l}_1}{\bar{l}_2}\right)\right]$$

which is approximately

$$0.3\times10^3\ \mathrm{sec}^{-2}$$

with

$$\frac{\bar{l}_1}{\bar{l}_2}=\frac{4B}{m_{\mathrm{Ga}}}\,\frac{1}{(\tilde{\omega}_{\mathrm{TA}}^2-4A/m_{\mathrm{Ga}})}\ ,$$

$$\Delta_1=\frac{1}{2}\left(\frac{1}{m_{\mathrm{P}}}-\frac{1}{m_{\mathrm{As}}}\right)$$

$$\Delta_2=\frac{1}{2}\left(\frac{1}{\sqrt{m_{\mathrm{P}}}}-\frac{1}{\sqrt{m_{\mathrm{As}}}}\right)\frac{1}{\sqrt{m_{\mathrm{Ga}}}}\ .$$

The calculated localized frequency for the crystal $GaP_{0.5}$ is $(\tilde{\omega}_{\mathrm{TA}}^2+\lambda_{\mathrm{TA}})^{1/2}=102\ \mathrm{cm}^{-1}$. This value and the value $\tilde{\omega}_{\mathrm{TA}}$ compare very well with the experimental ones which are for the crystals $GaP_{0.6}As_{0.4}$ $\tilde{\omega}_{\mathrm{TA}}=90\ \mathrm{cm}^{-1}$ and $\omega_{\mathrm{loc}}=105\ \mathrm{cm}^{-1}$.

Intuitively we can say that frequencies which are in the range of the common density of states are propagating waves. The highest propagating wave frequency is the VCA zone-edge mode. In addition we have a range of frequencies outside the common acoustical density of states. This range corresponds to short spatial correlation, and the wave propagation is limited to regions which correspond to GaP in the mixed crystal. This is the continuous range of localized states which peaks close to the $2\mathrm{TA}_X$(GaP) frequency.

On the other hand, at the center of the Brillouin zone, we observe in addition to the usual two-mode behavior, a peak which appears for small concentrations of As. This peak which is between the TO_Γ and LO_Γ of GaP has LO polarization.[14] Figure 2 shows the Raman-scattering spectra of $GaP_{0.95}As_{0.05}$ at 2 K showing clearly this peak. It corrresponds to the oscillation of phosphorus at the edge of the Brillouin zone which is made Raman active by the disorder.

For frequencies close to those of the Brillouin-zone edge, the density of states is the phonon band tail given by Eq. (49) which is deduced from case (b) and Eq. (39).

At the X point of the Brillouin zone, the LO(X) vibrations can be considered as one-dimensional vibrations. They depend almost solely on one force constant C, and they are expected to be more localized than the transverse modes.

Close to the $\omega_{\mathrm{LO}(X)}$ frequency we have

$$\mathrm{Im}\,G(X,X)_{\epsilon\to 0} \propto S^2 \exp\left(-\frac{S^3}{g_{\mathrm{eff}}}\right)$$

with

$$S^2 = \left(1 - \frac{\omega^2}{\omega^2_{\mathrm{LO(edge)}}}\right) ,$$

$$g_{\mathrm{eff}} = \frac{3}{32}\, \frac{\lambda^2_{\mathrm{LO}(X)}\, \gamma^{1/2}_{\mathrm{LO}(X)}}{\omega^3_{\mathrm{LO}(X)}}\, \mathrm{sech}^2\left[\tfrac{1}{2}\ln\left(\frac{z}{1-z}\right)\right] ,$$

in a one-dimensional crystal. Also,

$$\lambda_{\mathrm{LO}(X)} = \tfrac{4}{2} C\left(\frac{1}{M_{\mathrm{P}}} - \frac{1}{M_{\mathrm{As}}}\right) ,$$

$$\frac{4C}{M_{\mathrm{P}}} = \omega^2_{\mathrm{LO}(X)} = (404\ \mathrm{cm}^{-1})^2 .$$

For small As concentrations $z = 0.05$, we have

$$g_{\mathrm{LO}} \simeq 0.08\, \gamma^{1/2}_{\mathrm{LO}(X)}$$

with $\gamma^{1/2}_{\mathrm{LO}(X)}$ of the order of unity.

The density of states of the continuum of localized modes is maximum when

$$\frac{\partial}{\partial S}\, \mathrm{Im}\, G(X,X,\, S^2)_{\epsilon\to 0} = 0 ,$$

which gives

$$S^2 = \frac{4}{9}\, g^2_{\mathrm{eff}} = 0.002\gamma_{\mathrm{LO}} .$$

This shows that the localized density of states has a contribution close to the $\omega_{\mathrm{LO(edge)}}$ frequency. This explains the additional Raman peak observed below the $\omega_{\mathrm{LO}(\Gamma)}$ frequency.

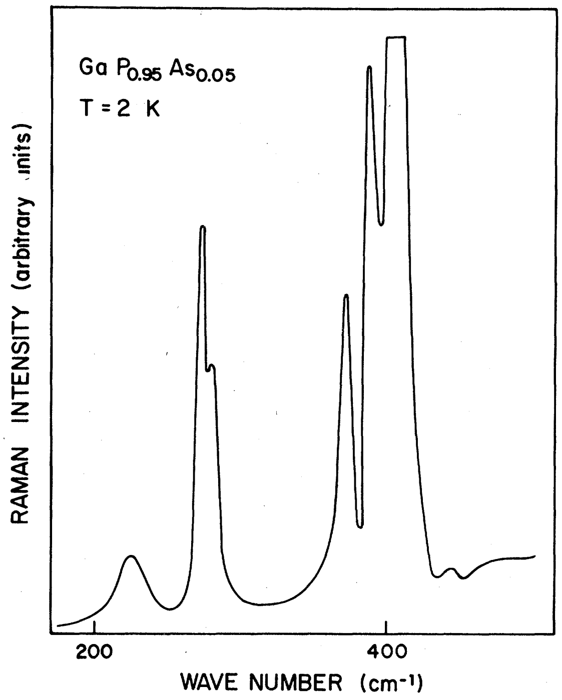

FIG. 2. Raman spectra at 2 K of $\mathrm{GaP_{0.95}As_{0.05}}$.

ACKNOWLEDGMENT

We want to thank Dr. D. M. Roessler from General Motors Research Laboratory for kindly providing the $\mathrm{GaP}_z\mathrm{As}_{1-z}$ crystals.

APPENDIX

We represent the two-point correlation function by the function derivative

$$G_{\alpha\alpha'}(l,l';\omega^2) = \frac{\delta}{\delta J_\alpha(l)}\, \frac{\delta}{\delta J_{\alpha'}(l')}\, \exp\left(\tfrac{1}{2} \sum_{\alpha l,\, \alpha' l'} J_{\alpha'}(l) G_{\alpha\alpha'}(l,l';\omega^2) J_{\alpha'}(l')\right)\Bigg|_{\vec{J}=0} , \tag{A1}$$

where $\vec{J} = (J_1(1),\ J_2(1), \ldots, J_1(N^3) J_2(N^3))$. We use the Gaussian transformation for a discrete number of variables, which appear in one dimension

$$\exp\left(-\frac{1}{4a^2}X^2 + SX\right) dX = \mathrm{const} \times \exp(a^2 S^2) \tag{A2}$$

and can be generalized to read in our case

$$\int_{-\infty}^{\infty} [du] \exp\left[-\left(\tfrac{1}{2} \sum_{\alpha l,\, \alpha' l'} u_\alpha(l)(\omega^2 - D)_{\alpha l,\, \alpha' l'} u_{\alpha'}(l') - \sum_{\alpha l} J_\alpha(l) u_\alpha(l)\right)\right]$$

$$= \mathrm{const} \times [\det(\omega^2 - D)]^{-1/2} \exp\left(\tfrac{1}{2} \sum_{\alpha l,\, \alpha' l'} J_\alpha(l)(\omega^2 - D)^{-1}_{\alpha l,\, \alpha' l'} J_{\alpha'}(l')\right) . \tag{A3}$$

Substituting $J = 0$ we obtain the known functional representation of a determinant

$$[\det(\omega^2 - D)]^{-1/2} \times \mathrm{const} = \int_{-\infty}^{\infty} [du] \exp\left(\tfrac{1}{2} \sum_{\alpha l,\, \alpha' l'} u_\alpha(l)(\omega^2 - D)_{\alpha l,\, \alpha' l'} u_{\alpha'}(l')\right) . \tag{A4}$$

From (A1) and (A3) we obtain the two-point correlation function in functional form

$$G_{\alpha\alpha'}(l,l';\omega^2)=Z^{-1}\frac{\delta}{\delta J_{\alpha'}(l')}\int_{-\infty}^{\infty}[du]\exp-\left(\frac{1}{2}\sum_{\alpha l,\,\alpha' l'}u_\alpha(l)(\omega^2-D)_{\alpha l,\,\alpha' l'}u_{\alpha'}(l')-\sum_{\alpha l}J_\alpha(l)u_\alpha(l)\right)\Bigg|_{\vec{J}=0}. \tag{A5}$$

$$G_{\alpha\alpha'}(l,l';\omega^2)=Z^{-1}\int_{-\infty}^{\infty}[du]u_\alpha(l)u_{\alpha'}(l')\exp\left(-\frac{1}{2}\sum_{\alpha l,\,\alpha' l'}u_\alpha(l)(\omega^2-D)_{\alpha l,\,\alpha' l'}u_{\alpha'}(l')\right). \tag{A6}$$

For more details on functional representation of the Green's function we refer to Amit.[13]

---

[1] E. N. Economou, M. H. Cohen, K. F. Freed, and E. S. Kirkpatrick, in *Amorphous and Liquid Semiconductors*, edited by J. Tauc (Plenum, New York, 1974).

[2] A. Nitzan, K. F. Freed, and M. H. Cohen, Phys. Rev. B 15, 4476 (1977).

[3] V. Emery, Phys. Rev. B 11, 231 (1975).

[4] E. Berezin, J. C. LeGuillou, and J. Zinn-Justin, Phys. Rev. D 15, 1544 (1977).

[5] J. L. Cardy, J. Phys. C 11, L321 (1978).

[6] I. F. Chang and S. S. Mitra, Adv. Phys. 20, 351 (1971).

[7] Y. S. Chen, W. Shockley, and G. L. Pearson, Phys. Rev. 151, 715 (1966).

[8] D. Schmeltzer, R. Beserman, and D. Slamoviths, Phys. Rev. B (1980) (in press).

[9] R. J. Elliott, J. A. Krumhansl, and P. L. Leath, Rev. Mod. Phys. 46, 465 (1974).

[10] J. S. Langher, Ann. Phys. (N.Y.) 41, 108 (1967).

[11] N. H. Christ and T. D. Lee, Phys. Rev. D 12, 1606 (1975).

[12] A. A. Maradudin, G. A. Weiss, and W. Jephsen, J. Math. Phys. (N.Y.) 2, 345 (1960).

[13] D. J. Amit, *Field Theory, the Renormalization Group and Critical Phenomena* (McGraw-Hill, New York, 1978).

[14] N. D. Strahm and A. L. McWhorter, *Light Scattering Spectra of Solids*, edited by G. W. Wright (Springer, New York, 1969), p. 455.